Jurnal Tribologi 46 (2025) 1-12

MYTRIBOS Malaysian Tribology Society

Jurnal Tribologi

Website : jurnaltribologi.mytribos.org e-issn: 2289-7232

CFD analysis of textured journal bearing for performance parameters

Nadia Nurul Nabihah Ahmad Fuad [1], Mohamad Ali Ahmad [1*], Jaharah A Ghani [2]

[1] Faculty of Mechanical Engineering, Universiti Teknologi MARA, 40450 Shah Alam, Selangor, MALAYSIA.
[2] Department of Mechanical and Manufacturing Engineering, Faculty of Engineering and Built Environment, Universiti Kebangsaan Malaysia, 43600 UKM Bangi, Selangor, MALAYSIA.
*Corresponding author: mohama9383@uitm.edu.my

KEYWORDS

Pressure profile
Coupling system
Surface texturing
Load carrying capacity

ABSTRACT

Surface texture technology offers improvements in mechanical and tribological properties. This study analyzed the effects of the dimple texture on the journal bearing surface compared to plain surface bearing. Dimple texturing parameters were tested on 5 different dimple shapes, different aspect ratio (0.25, 0.35, and 0.45), and different dimple arrays (parallel to the oil flow and perpendicular to the oil flow). The area ratio of the dimple was fixed to 5%. The coupling system simulation was run using ANSYS software to obtain the results needed. The results show that the presence of a dimple texture on the bearing surface can improve the journal bearing performance by having less pressure, which reduces the friction compared to a plain surface. Additionally, by having turbulence oil flow, it's given more load capacity to the journal bearing performance.

1.0 INTRODUCTION

Journal bearings are one of the common mechanical components. Their function is to transmit energy and power by supporting rotating shafts that carry loads. Eccentricity ratio can impact how the load is distributed across the bearing. It also influences how the lubrication layer forms between the surfaces to prevent wear. If the ratio is too high or too low, it affects the bearing's stability during operation, which can cause vibrations and failure. As a result, having the optimum ratio helps to maintain the proper clearance between the shaft and the bearing, minimizing uneven wear and short life. This load-carrying capacity is strongly related to pressure distribution

Received 29 July 2024; received in revised form 28 April 2025; accepted 16 May2025. To cite this article: Ahmad et al. (2025). CFD analysis of textured journal bearing for performance parameters. Jurnal Tribologi 46, pp.1-12.

in the critical section, which is called the wedge area, where the minimum film thickness is located. The basic design of a journal bearing already could reduce friction, as shown in Figure 1.

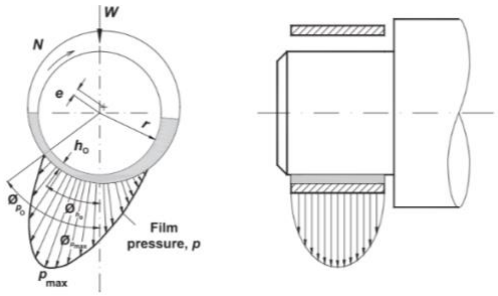

Figure 1: Motion of journal bearing generates pressure in hydrodynamic states (Keith, 1990).

W – load (N)
N – shaft rotation (rpm)
e – eccentricity (mm)
r – shaft radius (mm)
h_0 – film thickness (mm)
$Ø_{P0}$ – position of film termination (°)
$Ø_{h0}$ – position of minimum film thickness (°)
$Ø_{Pmax}$ – position of maximum pressure (°)
P_{max} – maximum pressure distribution (Pa)

However, studies show that the presence of surface texturing can improve friction resistance and appropriately adjust the flow gap (Gu et al., 2024). One of the famous surface-texturing technologies is dimple. It can improve tribological performance such as reducing friction, increasing load-carrying capacity, and lowering wear resistance while also lowering energy consumption [(Etsion & Burstein, 1996), (Etsion et al., 1999), (Ronen et al., 2001), (Brizmer et al., 2003), (Tala-Ighil et al., 2011), (Lu & Wood, 2020)] by acting as a reservoir that also traps wear debris during operation.

Besides, the dimples create a micro-hydrodynamic effect, which means they can help generate additional pressure in the lubricant coating. When the journal rotates, the lubricant spreads across the surface, and the dimples contribute to pressure buildup. This increased pressure lifts the journal and boosts load-carrying capacity by supporting it with a thicker coating of lubricant rather than face-to-face contact with the bearing surface. The dimples are designed to uniformly transmit pressure throughout the bearing's surface. This eliminates excessive pressure concentration at a few locations, which could otherwise cause friction and wear, as well as lubricant breakdown.

Referring to past studies [(X. Wang et al., 2015), (Yu et al., 2010)], some of the key parameters that were significant to the dimple texturing were dimple shape, area ratio, aspect ratio, and dimple array on surface. The area ratio, or else known as dimple density, is defined as a ratio between dimple area and overall surface area, whereas aspect ratio is the ratio between diameter and depth of the dimple (Ibatan et al., 2015). Besides that, the idea of having partially surface

texturing instead of fully surface texturing on the bearing can create converging clearance effectively (Cohen & Goltsberg, 2023).

By using computational fluid dynamics simulation, many complex problems can be analyzed. In real-life tests, it is limited to certain parameters and some quantities that can be measured. While using CFD analysis, all desired quantities can be measured at once and with high resolution in space and time. There are two equations that are often used by researchers to test or study dimple texturing performance. The Reynold's equation that is a half differential equation that involves pressure distribution on lubrication film and the Navier-Stoke's equation that simplified the Reynolds's equation as Equation (1).

$$\frac{d}{dx}\left(h^3\frac{dp}{dx}\right)+\frac{d}{dy}\left(h^3\frac{dp}{dy}\right)=6\mu U\frac{dh}{dx}+12\mu U\frac{dh}{dt} \quad (1)$$

The left side term represents fluid analysis of pressure generation, while the right-side term represents fluid analysis of shear. Where h is fluid film thickness, p is average hydrodynamic pressure, x and y are coordinates, μ is fluid viscosity, and U is surface velocity (Etsion, 2013).

While Navier-Stoke's equation is a complex equation of Reynold where rate of velocity changes was added due to changes in fluid velocity that occur from one area to another. A continuity equation is also included in this equation to preserve the fluid mass in the flow of the fluid. In the steady and compact state, fluid flow can be assumed as Equation (2) and for continuity equation as Equation (3).

$$\rho(u.\nabla)u=-\nabla p+\nabla.(u\nabla u) \quad (2)$$

$$\nabla.u=0 \quad (3)$$

With u is the velocity vector at x, y, and z coordinates, ρ is fluid density, μ is fluid viscosity, and p is fluid pressure. This Navier-Stoke's and continuity equation had been resolved through commercial computational fluid dynamics (CFD) software (Li et al., 2017). Navier-Stokes is also able to describe 3D flow accurately (Rom & Müller, 2018) and employ much finer mesh (Christiansen et al., 2017).

Therefore, in this study, the effects of different shapes and arrays on the journal bearing surface on the pressure distribution were analyzed using coupling system model in computational fluid dynamics (CFD) simulation.

2.0 EXPERIMENTAL PROCEDURE

In this paper, a typical 3-dimensional journal bearing model was developed using the ANSYS software. 12 tiny holes were designed on the middle surface of the bearing to represent the transducer sensor location. The holes were placed 30° apart from each other. The lubricating oil used is hydraulic oil with a density of 860 kg/m^3 and a viscosity of 0.05848 kg/ms. Table 1 shows the parameters of the journal bearing based on the Raimondi and Boyd chart. The bearing characteristics number, S, was assumed to be 0.14 then the eccentricity ratio, $\varepsilon=\frac{h_0}{C}=0.44$. This selection of eccentricity ratio is acceptable considering the actual eccentricity was 0.22mm which is less than the radial clearance, which is 0.5 mm. It is avoiding the possibility of dry contact between bearing and shaft that leads to high friction by having thin layer of lubricant in between.

Then, the position of the maximum pressure, $Ø_{Pmax}$, was calculated as 18.5°, where the dimples were located. For references, 3 dimple designs from previous research were studied to find the best dimple design for journal bearing. The reference dimple parameters were shown in Table 2. All the dimples were designed with a 5% area ratio and the positioning of each dimple on the bearing surface as shown in Figure 2.

Table 1: Parameters of journal bearing.

Parameters	Descriptions/values
Bearing length (mm)	100
Shaft length (mm)	99
Radial clearance (mm)	0.5
Attitude angle (°)	54
Bearing load (kN)	6.12
Position of minimum film thickness (°)	54
Position of film termination (°)	77

Table 2: Reference dimple parameters.

Study No	Diameter	Depth (mm)	Aspect ratio	Reference
1	4mm	0.2	0.05	(Kumar Gupta et al., 2013)
2	4mm, 1mm	1.04	0.26	(Murthy & Raghunandana, 2018)
3	2mm, 2mm	0.5	0.25	(Y. Wang et al., 2023)

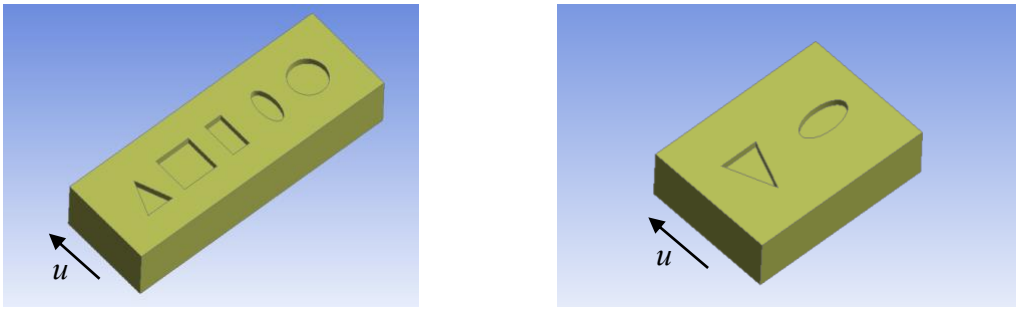

(a) (b)

Figure 2: Dimple array on bearing surface (a) parallel to the oil flow (b) opposite to the oil flow. *u* represent the lubricant flow.

Once the best design of dimple was determined, it was modified to several shapes. To focus on the effects of other dimple shapes and dimple arrays on the journal bearing performance, the area of dimple and the dimple area ratio were fixed in this study. Table 3 shows the modification parameters of the selected dimple design.

Table 3: Modifications parameters of the dimple design.

Parameters	Descriptions
Dimple shape	Circle, ellipse, triangle and rectangle
Aspect ratio	0.25, 0.35 and 0.45
Dimple array on bearing	Parallel to the oil flow and opposite to the oil flow

The modified designs of dimple were then simulated in computational fluid dynamics (CFD) using a coupling system. This model combines the governing equations of the individual physical phenomena involved, with the objective of capturing their interactions such as fluid flow, solid mechanics and thermal dynamics. First, the journal bearing was modelled as Figure 3 in transient structural; then, a meshing process was done to each of the journal bearings with a dimple design in fluid flow (fluent). This process was a crucial part of obtaining more detailed readings for the simulations. Meshing parameters that were tabulated in Table 4 were a default setting to maintain the consistency of the meshing reading. While Figure 4 shows the meshed bearing with and without dimple texture on the surface.

Key mathematical models used to describe fluid motion were momentum Equation (Navier-Stokes) as Equation (4) and energy equation for heat transfer as Equation (5) and the convergence tolerance was $1.0\times e^{-6}$ to avoid any inaccurate reading and ensure the quality during the meshing. As for solid mechanics, the governing equation of deformation is used as Equation (6), Equation (7) and Equation (8).

$$\frac{\partial \rho u}{\partial t} + \nabla.(\rho uu) = -\nabla p + \nabla.\tau + f \tag{4}$$

Where, ρ is the fluid density, p is pressure, τ is the viscous stress tensor and f is the body force.

$$\frac{\partial(\rho E)}{\partial t} + \nabla.\big(u(\rho E + p)\big) = \nabla.(k\nabla T) + Q \tag{5}$$

Where, E is total energy per unit mass, k is thermal conductivity, T is temperature and Q represent the heat sources.

$$\nabla.\sigma + f = 0 \tag{6}$$

$$\sigma = C:\epsilon \tag{7}$$

$$\epsilon = \frac{1}{2}(\nabla u + (\nabla u)^T) \tag{8}$$

Where, σ is the stress tensor, f is the body force, C is the stiffness matrix, ϵ is the strain tensor and u is the displacement vector.

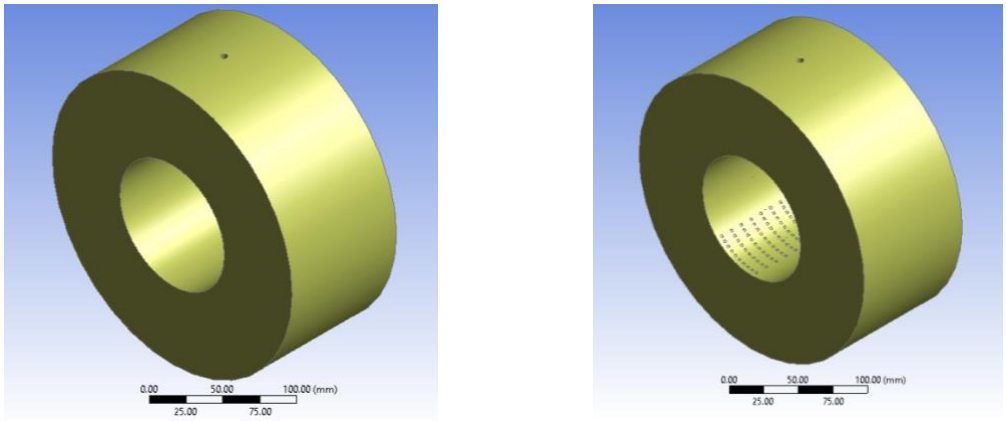

(a) (b)

Figure 3: Bearing model of (a) plain bearing (b) square dimple textured bearing.

Table 4: Meshing parameters.

Parameters	**Descriptions/values**
Span angle center sizing	Coarse
Transition sizing	Fast
Inflation option	Smooth transition
Smoothing quality	Medium
Transition ratio	0.272
Growth rate	1.2
Maximum layers	5

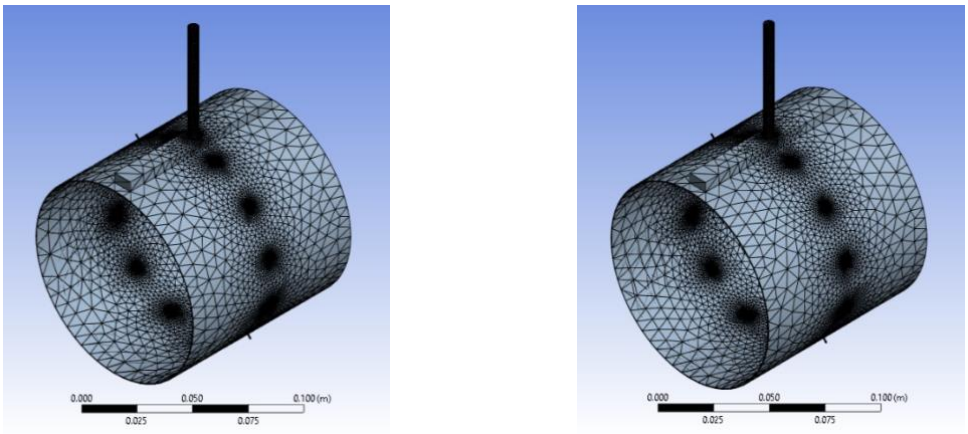

(a) (b)

Figure 4: Fluent meshing of (a) plain bearing (b) square dimple textured bearing

After the meshing process was done, parameters for the coupling system were set up to complete the simulation process. The time step was set to 50s with an iteration of 5 times. In this model, the mathematical model used were fluid domain and structure domain as Equation (9) and

Equation (10) respectively. In this, kinematic (for displacement) and dynamic (for stress) boundary condition were taken into consideration.

$$\nabla . u = 0, \frac{\partial u}{\partial t} + \nabla . (uu) = -\nabla p + \mu \nabla^2 u + f \quad (9)$$

$$\nabla . \sigma = f \quad (10)$$

Where, u is displacement vector, σ is stress tensor and f is body force.

3.0 RESULTS AND DISCUSSION

The results of the simulation were analyzed once the coupling system was completed. Figure 5 shows the results on the pressure contouring for the reference study compared to the plain bearing surface.

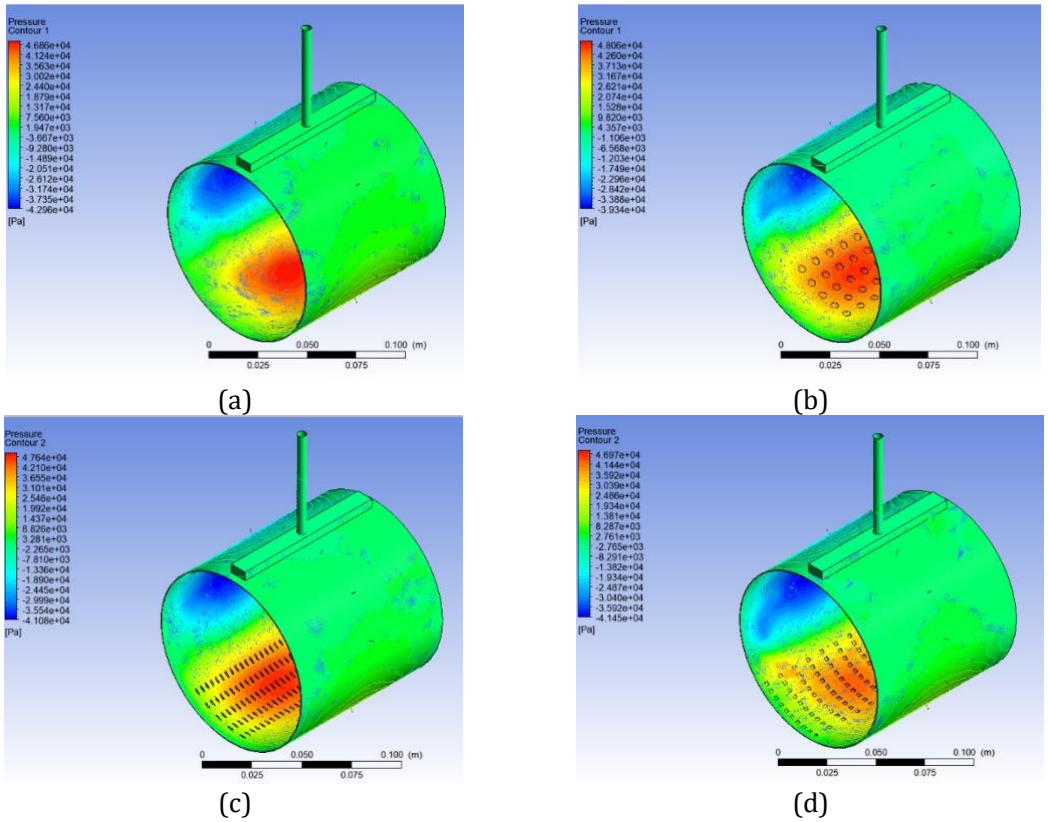

Figure 5: Pressure contouring for reference study compared to plain bearing (a) plain bearing (b) Study No 1 (c) Study No 2 (d) Study No 3.

It was observed that the pressure was directed to the lower part of the bearing where the wedge gap was located. It was proved by the calculation made from the Raimondi and Boyd chart that the maximum pressure, $Ø_{Pmax}$, was calculated as 18.5°.

From the analysis, it shows that bearing with Study No 3 that using square dimple shape has the lowest pressure reading with 41.44 kPa compared to 48.73 kPa reading for plain surface bearing and the other two references. Next, Figure 6 shows the pressure contouring results for the modifications of the square dimple parameters on the bearing.

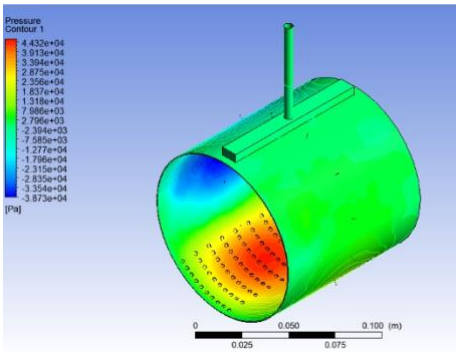

(a)

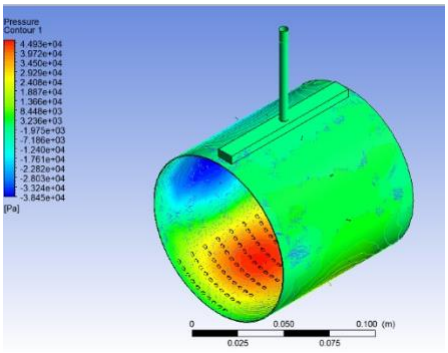

(b)

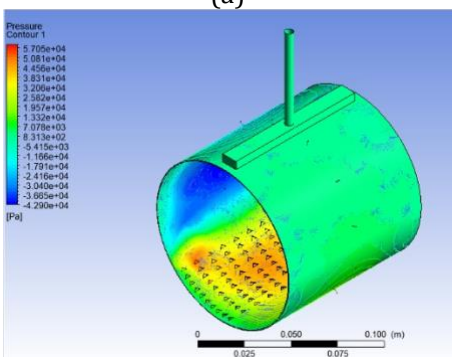

(c)

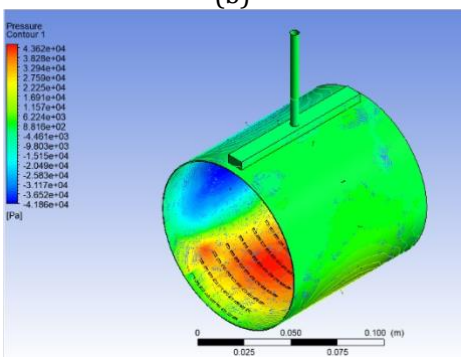

(d)

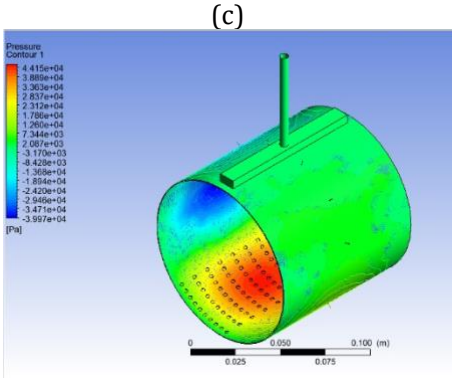

(e)

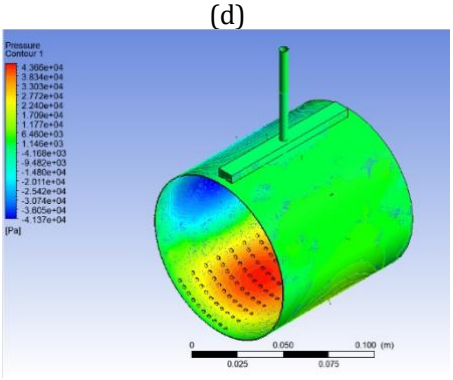

(f)

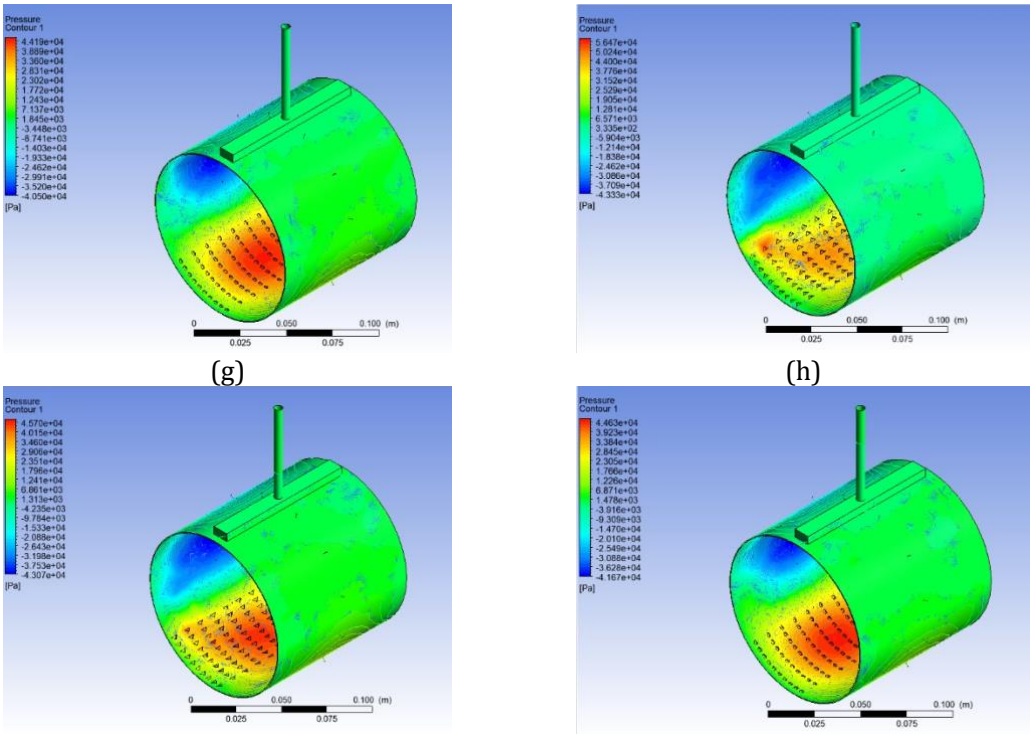

(g) (h)

(i) (j)

Figure 6: Pressure contouring for modification of Study No 3 bearing (a) Parallel circle 0.25 (b) Parallel ellipse 0.25 (c) Parallel triangle 0.25 (d) Parallel rectangle 0.25 (e) Perpendicular ellipse 0.35 (f) Parallel circle 0.35 (g) Parallel ellipse 0.35 (h) Parallel triangle 0.35 (i) Perpendicular triangle 0.35 (j) Parallel ellipse 0.45.

Then, pressure profile readings around the bearing surface were plotted. Figure 7 shows the comparison of pressure readings for all types of bearing surfaces. The highest-pressure readings for all types of journal bearings were traced at angle 210°, where the place of minimum film thickness is. Then, the highest-pressure readings for all the bearing types were plotted in Figure 8.

Generally, Figure 8 shows the improvement of the pressure reading for the plain surface bearing compared to the textured surface bearing. The pressure reading for the textured bearing surface reduced to 46 kPa and below. When comparing the effects of aspect ratios in this study, it seems that the deeper the dimple depth, the lower the pressure reading. It is due to the dimple depth that acts as a reservoir and the high turbulence of the oil flow. However, at certain depths without enlarging the size of the diameter, the pressure might increase as for bearing with a parallel ellipse with a 0.45 aspect ratio dimple texture.

In addition, the shape of dimples in a journal bearing influences pressure distribution also load-carrying capability. While spherical and elliptical dimples normally increase hydrodynamic pressure due to their smooth curvature and moderate geometry changes, different with square dimples that have a distinct behavior. In my testing findings, square dimples yielded the lowest pressure among the other shapes. This result can be due to the sharp corners and flat edges of square geometry, which disrupt lubricant flow more severely than round geometries. These

sudden shifts are likely to generate early flow separation and, possibly micro-cavitation, both of which minimize the accumulation of hydrodynamic pressure.

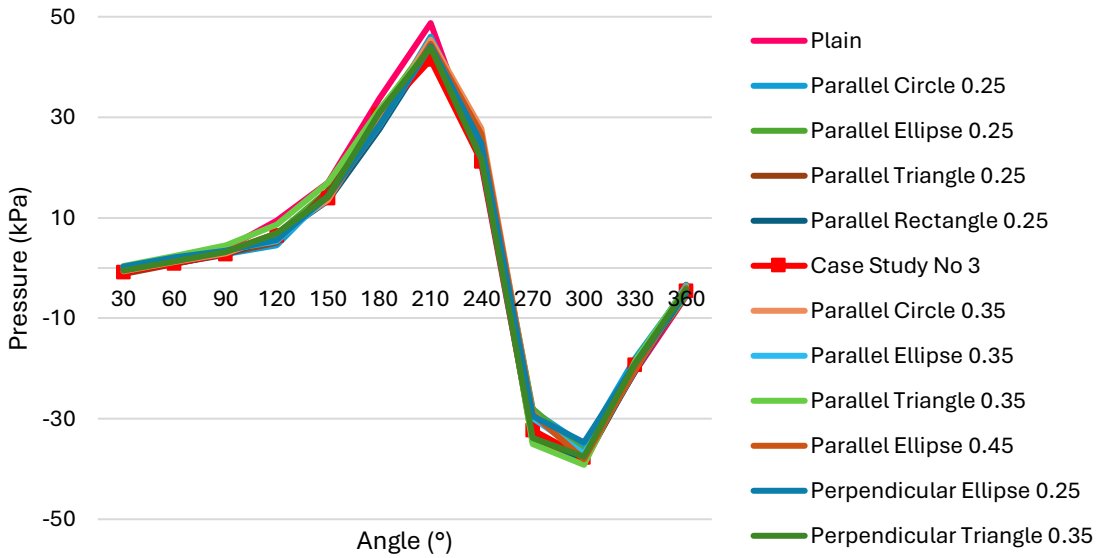

Figure 7: Pressure reading (kPa) for different type bearing surface with different aspect ratio.

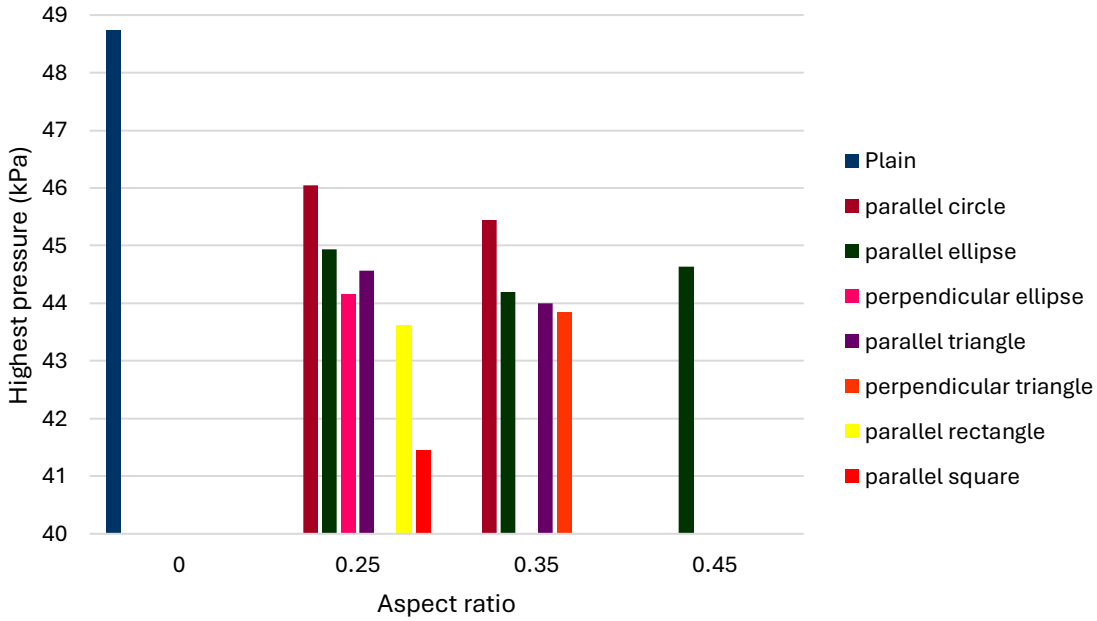

Figure 8: Highest-pressure readings for all the bearing types with different aspect ratios.

This finding emphasizes that not all textured surfaces increase bearing performance equally. Dimple shapes must be carefully chosen based on the intended pressure profile and operating conditions. Although texturing is meant to increase load capacity, certain shapes, such as square dimples, might have the reverse effect if not adjusted for flow behavior. This can be seen in the result that square dimple with 0.25 aspect ratio obtained the lowest pressure reading which is 41.44kPa. It was proven by (Y. Wang et al., 2023), that this square dimple design also shows the positive effects to the journal bearing performance in terms of pressure reading compared to other designs in the study. However, the square dimple is not suitable for designing for 0.35 and 0.45 aspect ratio.

In terms of journal bearing performance, low load with high speed is generally preferred for low friction and longer bearing life, whereas high load with low speed can cause increased wear due to insufficient lubrication. This study only focuses on a single speed (500rpm), so another study should be conducted to discover how varying speed and load can influence the behavior of the lubricating film, the bearing's stability, and the overall efficiency of the journal bearing.

CONCLUSIONS

In this paper, the authors have simulated several journal bearings with different dimple texture surfaces to compare with plain journal bearings using computational fluid dynamic analysis. The purpose of the simulation was to see if the presence of dimple texture on the bearing surface can improve the performance of journal bearings using coupling system analysis. The main results are summarized here:

(a) Bearings with dimple texture can improve the journal bearing performance.
(b) Square dimple texture was observed to be the best design in this study by reducing the pressure reading by 14% compared to plain surface bearing.
(c) Generally, having turbulence flow in journal bearing operation gives more load capacity, as mentioned by (Betti et al., 2022), also reduces the pressure distribution and friction between the surfaces.

REFERENCES

Betti, A., Forte, P., & Ciulli, E. (2022). Turbulence Effects in Tilting Pad Journal Bearings: A Review. Lubricants, 10(8). https://doi.org/10.3390/lubricants10080171

Brizmer, V., Kligerman, Y., & Etsion, I. (2003). A laser surface textured parallel thrust bearing. Tribology Transactions, 46(3), 397–403. https://doi.org/10.1080/10402000308982643

Christiansen, C. K., Walther, J. H., Klit, P., & Vølund, A. (2017). Investigation of journal orbit and flow pattern in a dynamically loaded journal bearing. Tribology International, 114(January), 450–457. https://doi.org/10.1016/j.triboint.2017.04.013

Cohen, I., & Goltsberg, R. (2023). Partial Surface Texturing in Hydrodynamic Lubrication: A CFD-Based Investigation. Lubricants, 11(9). https://doi.org/10.3390/lubricants11090395

Etsion, I. (2013). Modeling of surface texturing in hydrodynamic lubrication. Friction, 1(3), 195–209. https://doi.org/10.1007/s40544-013-0018-y

Etsion, I., & Burstein, L. (1996). A model for mechanical seals with regular microsurface structure. Tribology Transactions, 39(3), 677–683. https://doi.org/10.1080/10402009608983582

Etsion, I., Kligerman, Y., & Halperin, G. (1999). Analytical and experimental investigation of laser-textured mechanical seal faces. Tribology Transactions, 42(3), 511–516.

https://doi.org/10.1080/10402009908982248

Gu, C., Cui, Y., & Zhang, D. (2024). Research on the Optimal Design Approach of the Surface Texture for Journal Bearings. Lubricants, 12(4). https://doi.org/10.3390/lubricants12040111

Ibatan, T., Uddin, M. S., & Chowdhury, M. A. K. (2015). Recent development on surface texturing in enhancing tribological performance of bearing sliders. Surface and Coatings Technology, 272(November 2017), 102–120. https://doi.org/10.1016/j.surfcoat.2015.04.017

Keith, T. G. (1990). Journal bearings. https://doi.org/10.1142/9781848161856_0008

Kumar Gupta, K., Kumar, R., Kumar, H., & Sharma, M. (2013). Study on Effect of Surface Texture on the Performance of Hydrodynamic Journal Bearing. International Journal of Engineering and Advanced Technology (IJEAT), 3, 49.

Li, K., Jing, D., Hu, J., Ding, X., & Yao, Z. (2017). Numerical investigation of the tribological performance of micro-dimple textured surfaces under hydrodynamic lubrication. Beilstein Journal of Nanotechnology, 8(1), 2324–2338. https://doi.org/10.3762/bjnano.8.232

Lu, P., & Wood, R. J. K. (2020). Tribological performance of surface texturing in mechanical applications-a review. Surface Topography: Metrology and Properties, 8(4). https://doi.org/10.1088/2051-672X/abb6d0

Murthy, A. A., & Raghunandana, D. (2018). Study of Dimple Effect on the Friction Characteristics of a Journal Bearing using Taguchi Method. IOP Conference Series: Materials Science and Engineering, 314(1). https://doi.org/10.1088/1757-899X/314/1/012014

Rom, M., & Müller, S. (2018). An effective Navier-Stokes model for the simulation of textured surface lubrication. Tribology International, 124(February), 247–258. https://doi.org/10.1016/j.triboint.2018.04.011

Ronen, A., Etsion, I., & Kligerman, Y. (2001). Friction-reducing surface-texturing in reciprocating automotive components. Tribology Transactions, 44(3), 359–366. https://doi.org/10.1080/10402000108982468

Tala-Ighil, N., Fillon, M., & Maspeyrot, P. (2011). Effect of textured area on the performances of a hydrodynamic journal bearing. Tribology International, 44(3), 211–219. https://doi.org/10.1016/j.triboint.2010.10.003

Wang, X., Wang, J., Zhang, B., & Huang, W. (2015). Design principles for the area density of dimple patterns. Proceedings of the Institution of Mechanical Engineers, Part J: Journal of Engineering Tribology, 229(4), 538–546. https://doi.org/10.1177/1350650114531939

Wang, Y., Jacobs, G., König, F., Zhang, S., & von Goeldel, S. (2023). Investigation of Microflow Effects in Textures on Hydrodynamic Performance of Journal Bearings Using CFD Simulations. Lubricants, 11(1). https://doi.org/10.3390/lubricants11010020

Yu, H., Wang, X., & Zhou, F. (2010). Geometric shape effects of surface texture on the generation of hydrodynamic pressure between conformal contacting surfaces. Tribology Letters, 37(2), 123–130. https://doi.org/10.1007/s11249-009-9497-4